Theory of the singly quasidegenerate Josephson junction parametric amplifier

Sørensen, O.H.; Dueholm, B.; Mygind, Jesper; Pedersen, Niels Falsig

Published in:
Journal of Applied Physics

Link to article, DOI:
10.1063/1.327507

Publication date:
1980

Document Version
Publisher's PDF, also known as Version of record

Theory of the singly quasidegenerate Josephson junction parametric amplifier

O. H. Soerensen, B. Dueholm, J. Mygind, and N. F. Pedersen
Physics Laboratory I, The Technical University of Denmark, DK-2800 Lyngby, Denmark

(Received 8 January 1980; accepted for publication 4 April 1980)

A comprehensive account of the theory of the singly quasidegenerate Josephson junction parametric amplifier is given. In this mode the signal and idler frequencies are both approximately equal to half the pump frequency, and hence the signal and idler channels have a common termination. It is shown that the performance of the amplifier characterized by properties such as gain-bandwidth product, noise temperature, and saturation depends strongly on the embedding microwave circuit. In particular any uncompensated series reactance may deteriorate the overall performance. Internal shot and Johnson noise as well as incident thermal radiation is included in the discussion. It is shown that the noise temperature is virtually independent of noise injected from external sources and that minimum noise temperature is automatically achieved if the amplifier is tuned to maximize the gain-bandwidth product. The analytical results are illustrated by self-consistent numerical solutions of the circuit equations.

PACS numbers: 74.50. + r, 74.30.Gn, 84.30.Dx, 85.25. + k

I. INTRODUCTION

Josephson junction parametric amplifiers have been studied extensively—theoretically and experimentally—in the recent years. Three different modes of operation—two externally pumped and one internally pumped—have been considered.

The latter mode of parametric amplification which is unique for Josephson junctions has fairly bad noise properties due to the large spectral width of the internal Josephson oscillations used to pump the amplifier. Amplifier noise temperatures close to the theoretical limit of 42 times the ambient temperature, has been reported at X-band frequencies.[1,2] The doubly degenerate—or four wave—mode with external pump has been treated in a number of papers. Here, unbiased or magnetically biased Josephson junctions are used. The almost coinciding pump and signal frequencies allows for relatively simple microwave circuits and good noise performance with considerable gain has been obtained. With arrays of microbridges[3,4] or tunnel junctions[5,6] or with a single point contact[7] noise temperatures below 50 K were achieved at X band and in the 35-GHz band. A detailed theory has been formulated[8,9] which accounts well for the observations except for two important features. The gain-bandwidth product is invariably found much smaller than the theory predicts and the noise temperature often is much higher than expected. This high device noise has been suggested as caused by the phase fluctuation noise appearing when the stable limit cycle disappears at the operating point of the amplifier.[10]

A noise rise is often seen also in the singly degenerate—or three wave—mode of operation which is the subject of this paper. Also in this case the noise rise may be due to an instability of the operating point, although of a different nature. Experimentally, the singly degenerate mode has been studied at X band[11] and at 35 GHz.[12] At X band high gain and a very high noise temperature were found whereas moderate gain (less than 10 dB and noise temperatures below 100 K were achieved at 35 GHz. We shall include some comments on this problem when the paper is summarized in Sec. V.

The purpose of the paper is to give a detailed account of the theory of the singly quasidegenerate Josephson junction parametric amplifier. Two features of particular importance for the amplifier performance must be taken into account.

(i) The embedding microwave circuit has a strong influence on the amplifier properties which has not been given proper attention in previous work on Josephson junction parametric amplifiers. We shall point out that many of the so far unexplained experimental results may be understood as a result of the interaction with even simple external circuits.

(ii) The Josephson junction amplifier is very easily saturated which is a consequence of the extremely low pump power level necessary to operate the amplifier. Even at cryogenic temperatures the thermal fluctuation noise may cause a non-negligible saturation. The degree of saturation due to external sources (monochromatic or broad-band) may be reduced by using arrays of junctions since the available power is then distributed between the individual junctions. However, the internally generated thermal noise is not necessarily reduced in this way, and hence the theory must take saturation into account.

The paper is organized as follows: In Sec. II the theory of the singly degenerate mode is described. The admittance matrix of the nonlinear Josephson device which relates currents and voltages at the signal and idler frequencies is derived. The embedding microwave circuit is described and a prototype equivalent circuit which is sufficiently general to incorporate a broad class of realistic microwave circuits is selected. Based on an equivalent circuit model, expressions for amplifier properties such as input admittance, signal gain, and signal-to-idler conversion are derived. The results are too complicated to be evaluated by analytical methods except in special cases. One such case is the limit of high gain provided that the microwave circuit may be accounted for by a frequency independent impedance.

 0021-8979/80/105483-12$01.10

Section III presents the results of a numerical evaluation of a noise-free unsaturated amplifier, and in Sec. IV it is illustrated how external and internal noise modifies the response. First, the noise mechanisms to be taken into account are discussed and an analytical expression for the amplifier noise temperature is derived in the high gain limit. Second, the iteration scheme used to evaluate the performance of the saturated amplifier is outlined and illustrated in a few cases. Section V contains a summary and Sec. VI concludes the paper.

II. THEORY

A. The junction equations

The present derivation of the Josephson junction equations is based on the method introduced by Feldman in the doubly degenerate case.[9] In the singly degenerate mode we have a frequency relation between signal, idler, and pump frequencies: $\omega + \omega' = \omega_p$, where the signal frequency ω and the idler frequency ω' are about half the pump frequency $\omega \simeq \omega' \simeq \frac{1}{2}\omega_p$. Furthermore, a dc-bias current is introduced in order to drive the device into the parametrically active state. Finally, due to the separation of signal and idler frequencies from the pump frequency two independent input circuits must be used.

In order to simplify the calculation it is assumed that the junction is short circuited at all frequencies except the pump frequency and the frequencies in a band centered at half the pump frequency where the device may exhibit parametric gain. Then the junction voltage may be written in the form

$$V(t) = V_p \cos\omega_p t + V\cos(\omega t + \theta) + V'\cos(\omega' t + \theta') + \sum_k [V_k \cos(\omega_k t + \theta_k) + V_k' \cos(\omega_k' t + \theta_k')], \tag{1}$$

where the pump, signal, and idler components have amplitudes V_p, V, and V', and phases θ and θ' referred to the pump. The summation over k models the noise voltage and is extended over all frequencies where the junction may sustain a voltage. Also here the primed terms are the idlers at $\omega_k' = \omega_p - \omega_k$ associated with the noise input at ω_k. The approximation of the continuous noise spectrum by a series of discrete terms is reasonably good if the frequency separation $d\omega_k = \omega_k - \omega_{k-1}$ is small compared to the amplifier bandwidth and if we let the amplitude V_k be determined by the available noise power in the interval $d\omega_k$. The combination frequencies $2(\omega_p - \omega_k)$, $2(\omega_p - \omega_k')$, $\omega_p + \omega_k$, $\omega_p + \omega_k'$, $2\omega_p - \omega_k$, and $2\omega_p - \omega_k'$, etc., are neglected. This is justified only if the frequencies in a band of width $\frac{1}{3}\omega_p$ centered at $\frac{1}{2}\omega_p$ are important.

In Eq. (1) we distinguish between the signal and noise components. The signal-idler pair may be incorporated as terms in the summation and are not written explicitly below. It should only be kept in mind that they have properties different from the fluctuating noise components. The noise amplitudes are characterized by a zero time average and a nonzero rms value and only corresponding signal and idler terms V_l, V_l' are correlated whereas all other correlation functions $\overline{V_l(t)V_m(t-\tau)}$ and $\overline{V_l(t)V_m'(t-\tau)}$ with $l \neq m$ are zero. Here, the bar indicates time averaged values.

The relation between the junction voltage and current is—within the framework of the shunted junction model[13]—determined by the differential equations

$$I = C\frac{dV}{dt} + \frac{1}{R}(1 + \epsilon\cos\phi)V + I_c \sin\phi, \tag{2}$$

$$V = \frac{\hbar}{2e}\frac{d\phi}{dt}, \tag{2'}$$

where the current is expressed as a sum of a capacitive, a resistive (phase-dependent), and a pair contribution.

The phase difference ϕ is found by integration of Eq. (1),

$$\phi = \phi_0 + \alpha_p \sin\omega_p t + \sum_k [\alpha_k \sin(\omega_k t + \theta_k) + \alpha_k' \sin(\omega_k' t + \theta_k')], \tag{3}$$

with

$$\alpha_l = 2eV_l/\hbar\omega_l, \quad l = p,k, \tag{3'}$$

where the signal-idler pair is included in the summation. The junction voltage may be eliminated between (2) and (2'). Introducing the maximum Josephson plasma frequency $\omega_0 = (2eI_c/\hbar C)^{1/2}$ and the quality factor $Q_0 = \omega_0 RC$ we get

$$\frac{I}{I_c} = \frac{1}{\omega_0^2}\frac{d^2\phi}{dt^2} + \frac{1 + \epsilon\cos\phi}{\omega_0 Q_0}\frac{d\phi}{dt} + \sin\phi. \tag{4}$$

The junction admittance elements are found by inserting Eq. (3) into Eq. (4) and Fourier expanding $\sin\phi$ and $\cos\phi\, d\phi/dt = d(\sin\phi)/dt$. To the lowest order which includes saturation we have, using an obvious notation, $\sin(\phi_0 + \phi_p + \Sigma_k) = \sin(\phi_0 + \phi_p)[1 - \frac{1}{2}(\Sigma_k)^2] + \cos(\phi_0 + \phi_p)[\Sigma_k - \frac{1}{6}(\Sigma_k)^3]$, where $\frac{\sin}{\cos}\Sigma_k$ are expanded to third order in $\Sigma_k \ll 1$. This step has been thoroughly discussed by Feldman.[9] Saturation appears as a shift in the static operating point, and only terms in the expansion with a nonzero time average contribute.

It turns out that the junction current depends on the noise through the combinations

$$A = \sum_k \left(\overline{|\alpha_k|^2} + \overline{|\alpha_k'|^2}\right), \tag{5}$$

$$B = \sum_k \overline{\alpha_k \alpha_k'}, \tag{5'}$$

where α_k and α_k' are the complex amplitudes at ω_k and ω_k', respectively. We shall use the complex notation throughout the remainder of the paper. Both A and $|B|$ must be small.

The Fourier expansion of $\sin\phi$ yields the following components at dc:

$$(1 - \tfrac{1}{4}A)J_0 \sin\phi_0 - \tfrac{1}{2}\mathrm{Im}B\, J_1 \cos\phi_0, \tag{6}$$

at ω_p:

$$-2j(1 - \tfrac{1}{4}A)J_1 \cos\phi_0, + \tfrac{1}{2}(J_0 B + J_2 B^*)\sin\phi_0, \tag{7}$$

at $\omega_k \neq \frac{1}{2}\omega_p$:

$$g_{11}\alpha_k + g_{12}\alpha_k'^*, \tag{8}$$

and at ω_k':

$$g_{12}\alpha_k^* + g_{11}\alpha_k', \tag{8'}$$

with

$$g_{11} = -j[(1-\tfrac{1}{4}A)J_0\cos\phi_0 + \tfrac{1}{2}\mathrm{Im}BJ_1\sin\phi_0], \tag{9}$$

$$g_{12} = -(1-\tfrac{1}{4}A)J_1\sin\phi_0 + j\tfrac{1}{4}(BJ_0 + B^*J_2)\cos\phi_0, \tag{9'}$$

where the argument α_p of the Bessel functions J_0, J_1, J_2 has been suppressed. The asterisks indicate complex conjugation.

The frequency component at $\omega_k = \omega_k' = \frac{1}{2}\omega_p$ needs special attention. It is known that the junction may break into large amplitude oscillations at this frequency if the pump power level exceeds a certain threshold value.[14] The third-order expansion in Σ_k used here becomes insufficient under such circumstances, and consequently we must assume that the amplifier is always operated below the threshold for the half-harmonic oscillation.

Adding the currents through the capacitive and resistive channels we find the total current. In terms of voltage rather than phase modulation we get

$$\frac{I_{dc}}{I_c} = (1-\tfrac{1}{4}A)J_0\sin\phi_0 - \tfrac{1}{2}\mathrm{Im}BJ_1\cos\phi_0, \tag{10}$$

$$\frac{I_p}{I_c} = (g_1\sin\phi_0 + g_2\cos\phi_0)\left(1 + j\epsilon\frac{\omega_p}{\omega_0 Q_0}\right) + \left(\frac{1}{R} + j\omega_p C\right)V_p, \tag{11}$$

where the short-hand notation,

$$g_1 = \tfrac{1}{2}(J_0B + J_2B^*), \tag{12}$$

$$g_2 = -2j(1-\tfrac{1}{4}A)J_1, \tag{12'}$$

has been introduced.

Finally, the signal-idler relations are determined by the matrix equation

$$\begin{pmatrix} I_k \\ I_k'^* \end{pmatrix} = \begin{pmatrix} Y_{11} & Y_{12} \\ Y_{21} & Y_{22} \end{pmatrix}\begin{pmatrix} V_k \\ V_k'^* \end{pmatrix}, \tag{13}$$

with

$$Y_{11} = \frac{1}{R} + j\omega_k C + \frac{\omega_0 Q_0}{R\omega_k}g_{11}\left(1 + j\epsilon\frac{\omega_k}{\omega_0 Q_0}\right),$$

$$Y_{12} = \frac{\omega_0 Q_0}{R\omega_k'}g_{12}\left(1 + j\epsilon\frac{\omega_k}{\omega_0 Q_0}\right), \tag{14}$$

$$Y_{21} = \frac{\omega_0 Q_0}{R\omega_k}g_{12}^*\left(1 - j\epsilon\frac{\omega_k'}{\omega_0 Q_0}\right),$$

$$Y_{22} = \frac{1}{R} - j\omega_k' C + \frac{\omega_0 Q_0}{R\omega_k'}g_{11}^*\left(1 - j\epsilon\frac{\omega_k'}{\omega_0 Q_0}\right).$$

The dependence of the Eqs. (6)–(14) on A and B is responsible for the device saturation. The quantities A and B are according to their definitions (5) and (5') given by the system noise integrated over frequency and depend on the amplifier operating point which in turn depends on the degree of saturation. Hence the junction equations are all interdependent. In order to solve the equations the constraints imposed by the embedding circuit have to be invoked. In the next section a circuit model is described which is a reasonably realistic prototype for a class of coupling structures.

B. The coupling circuit

The circuit by which the junction is coupled to the external waveguide line has two functions: (i) to perform the impedance transformation between waveguide and junction, and (ii) to compensate for spurious reactances, e.g., the series inductance of the narrow strips between which the junctions(s) is (are) formed. The latter may have a considerable magnitude and acts to effectively decouple the junction and the input line.

The Josephson tunnel junction is a low-impedance device at high frequencies due to the capacitive shunt which, however, may be resonated out taking advantage of the internal Josephson plasma resonance. A tunnel junction with an impedance at resonance of the order 10 Ω is readily made and even higher impedances may be realized using series arrays of junctions. The impedance transformation from the characteristic waveguide impedance (typically 300–500 Ω for conventional waveguide and 50 Ω for coaxial or microstrip lines) to the junction impedance may be accomplished, e.g., using a stepped impedance quarterwave transformer.

Compensation of the strip inductance may be accomplished in several ways. Here, single-frequency resonance compensation circuits are considered. Figures 1(a) and 1(b) present two circuits with the required properties. Figure 1(a) shows a cross section of a conventional waveguide circuit where an iris or similar inductive shunt[15] is introduced at a distance $\frac{1}{4}(2n+1)\lambda$ from the junction terminals. Figure 1(b) shows a stripline version where the compensating element is a capacitive gap[16] at a distance $\frac{1}{2}n\lambda$ from the junction.

Both circuits may be represented by the lumped element equivalent circuit in Fig. 1(c). The impedance

$$Z_s = r_s + j(X_s - 1/B_s) \tag{15}$$

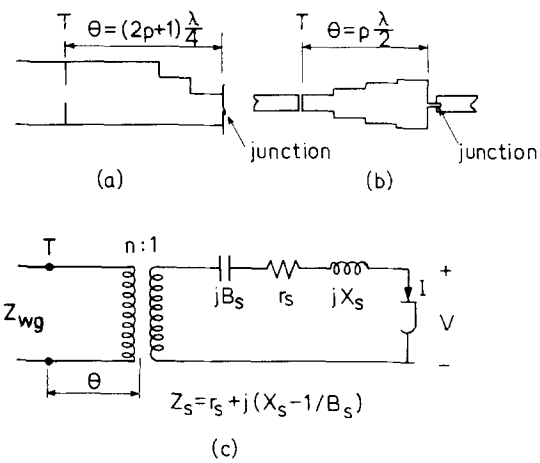

FIG. 1. Reflection amplifier circuits. (a) Conventional waveguide. (b) Stripline. (c) Equivalent circuit representation of (a) and (b) at terminals T. The series impedance Z_s depends on the specific circuit structure. The relation between I and V is given in Eqs. (2) and (2').

in series with the junction and the ideal n:1 transformator describes the coupling circuit. All losses are lumped together in the resistance r_s.

Using this equivalent circuit model the amplifier properties may be evaluated. Introducing $Z_0 = Z_{wg}/n^2$ we may express the incident and the reflected power at ω as

$$P^+ = \frac{1}{8Z_0}|(Z_s + Z_0)I + V|^2, \tag{16}$$

$$P^- = \frac{1}{8Z_0}|(Z_s - Z_0)I + V|^2, \tag{16'}$$

in terms of the junction current and voltage components at ω. Similar equations hold at the corresponding idler frequency, $\omega' = \omega_p - \omega$. Since no power is incident at ω' we have

$$0 = |(Z_s' + Z_0)I' + V'|^2, \tag{17}$$

$$P'^- = \frac{1}{8Z_0}|(Z_s' - Z_0)I' + V'|^2, \tag{17'}$$

where the prime as before indicates the quantities evaluated at the idler frequency. The signal power gain then is

$$G_{PA} \equiv \frac{P^-}{p^+} = \left| \frac{(Z_s - Z_0)Y_{in} + 1}{(Z_s + Z_0)Y_{in} + 1} \right|^2, \tag{18}$$

where the junction input admittance $Y_{in} = I/V$ has been introduced. The signal-to-idler conversion gain is readily found as the ratio P'^-/P^+. The input admittance is determined from the admittance matrix (13) and Eq. (17),

$$Y_{in} = Y_{11} - \frac{Y_{12}Y_{21}(Z_s'^* + Z_0)}{1 + Y_{22}(Z_s'^* + Z_0)}. \tag{19}$$

Hence the input admittance at the signal frequency depends on the complex conjugate of the coupling impedance at the idler frequency.

Since the pump frequency is about twice the signal frequency a separate pump circuit must be used. In the present context it is sufficient to assume that the pump signal is supplied from a line of characteristic impedance Z_p neglecting all spurious reactances. First, because the pump power requirement is sufficiently low that impedance mismatch at the pump frequency is not a serious problem with the power available from conventional microwave sources. Second, the frequency separation between the signal and pump bands allows for effective filtering such that reflected or transmitted pump power does not reach the mixer stage of the receiver. Hence the details of the pump circuit are not important and we shall assume that the operating point (ϕ_0, α_p) is determined from Eq. (10) and

$$P_p^+ = \frac{1}{8Z_p}|Z_p I_p + V_p|^2, \tag{20}$$

where I_p is given by Eq. (11) and V_p by Eq. (3'). This simplified description of the pump circuit prevents us from making a meaningful comparison between applied pump power and the signal or noise saturation level.

A complete picture of the amplifier is established by including system noise in a quantitative form as done in Sec. IV. It is obvious already at this point that numerical methods must be used in order to evaluate the equations in the general case. It is instructive, however, to consider the special case of high gain which under some circumstances may be approached by analytical methods.

C. The high-gain limit

The analysis is simplified considerably by assuming that a broad-band compensation of the series inductance X_s has been realized. This means that the series impedance becomes $Z_s = r_s$ independent of frequency over the bandwidth of the amplifier. Then the signal gain becomes, from Eqs. (18) and (19),

$$G_{PA} = \left| \frac{Z_0(Y_{11} - Y_{22}) - r_s(Y_{11} + Y_{22}) + (Z_0^2 - r_s^2)(Y_{11}Y_{22} - Y_{12}Y_{21}) - 1}{(Z_0 + r_s)(Y_{11} + Y_{22}) + (Z_0 + r_s)^2(Y_{11}Y_{22} - Y_{12}Y_{21}) + 1} \right|^2. \tag{21}$$

In the high-gain limit where the bandwidth is narrow it is sufficient to evaluate Eq. (21) to first order in the signal-to-idler separation $\Delta\omega = \omega - \omega'$. The matrix elements Y_{ij} are given in Eq. (14). It is convenient to introduce a frequency ω_R such that $g_{11} = -j(\omega_R/\omega_0)^2$, where

$$\omega_R = \omega_0[(1 - \tfrac{1}{4}A)J_0 \cos\phi_0 + \tfrac{1}{2}\,\mathrm{Im}B\,J_1 \sin\phi_0]^{1/2} \tag{22}$$

is a real positive quantity in all cases of interest. In the noise-free case ω_R is recognized as the Josephson plasma frequency. In order to save space we may put $\epsilon \doteq 0$ without changing the qualitative results.[13] After some calculation we find

$$\begin{aligned} G_{PA} = \Bigg| & (Z_0^2 - r_s^2)\left(1 + \left(\frac{\omega_0 Q_0}{\omega_c}\right)^2\left\{\left[\left(\frac{\omega_c}{\omega_0}\right)^2 - \left(\frac{\omega_R}{\omega_0}\right)^2\right]^2 - |g_{12}|^2\right\}\right) - 2r_s R - R^2 \\ & + j\left\{(Z_0^2 - r_s^2 - r_s R)\left[1 + \left(\frac{\omega_R}{\omega_c}\right)^2\right]Q_0\frac{\Delta\omega}{\omega_0} \right. \\ & \left. + 2Z_0 R\,\frac{\omega_0 Q_0}{\omega_c}\left[\left(\frac{\omega_c}{\omega_0}\right)^2 - \left(\frac{\omega_R}{\omega_0}\right)^2\right]\right\}\Bigg|^2 \Bigg/ \Bigg| (Z_0 + R + R_s)^2 + (Z_0 + r_s)^2\left(\frac{\omega_0 Q_0}{\omega_c}\right)^2\left\{\left[\left(\frac{\omega_c}{\omega_0}\right)^2 - \left(\frac{\omega_R}{\omega_0}\right)^2\right]^2 - |g_{12}|^2\right\} \\ & + j(Z_0 + r_s)(Z_0 + R + r_s)\left[1 + \left(\frac{\omega_R}{\omega_c}\right)^2\right]Q_0\frac{\Delta\omega}{\omega_0}\Bigg|^2. \end{aligned} \tag{23}$$

From Eq. (23) it is obvious that ω_R is a resonance frequency of the junction. The frequency ω_c also introduced in Eq. (23) is the centerband frequency $\omega_c = \frac{1}{2}\omega_p$ at which the gain is maximum ($\omega = \omega_c$ corresponds to $\Delta\omega = 0$). Infinite centerband gain results if the operating point satisfies

$$|g_{12}|^2 = \left(\frac{\omega_c}{\omega_0 Q_0}\right)^2 \left(\frac{Z_0 + R + r_s}{Z_0 + r_s}\right)^2 + \left[\left(\frac{\omega_c}{\omega_0}\right)^2 - \left(\frac{\omega_R}{\omega_0}\right)^2\right]^2, \tag{24}$$

with $|g_{12}|$ from Eq. (9'). Equation (24) defines the threshold curve for amplifier instability against oscillations at half the pump frequency.[14,17]

In the limit of high but finite gain the threshold condition may be inserted in the numerator of Eq. (23) and the centerband gain (at $\Delta\omega = 0$) simplifies to

$$G_{PA} = \frac{|2Z_0R\,[(Z_0 + R + R_s)/(Z_0 + r_s)] + j2Z_0R\,(\omega_0Q_0/\omega_c)[(\omega_c/\omega_0)^2 - (\omega_R/\omega_0)^2]\,|^2}{|(Z_0 + R + r_s)^2 + (Z_0 + r_s)^2(Q_0\omega_0/\omega_c)^2\{[(\omega_c/\omega_0)^2 - (\omega_R/\omega_0)^2]^2 - |g_{12}|^2\}\,|^2}. \tag{25}$$

The right-hand side of Eq. (24) is minimum at $\omega_c = \omega_R$, i.e., at the plasma resonance. Here, the bandwidth at half-maximum gain becomes, assuming that the $\Delta\omega$ dependence of the numerator in Eq. (23) is negligible compared to that of the denominator,

$$\Delta\omega_{PA} = \omega_0 \frac{(Z_0 + R + r_s)^2 - (Z_0 + r_s)^2(\omega_0Q_0/\omega_c)^2|g_{12}|^2}{2(Z_0 + R + r_s)(Z_0 + r_s)Q_0}. \tag{26}$$

The gain-bandwidth product may be written

$$G_{PA}^{1/2}\Delta\omega_{PA} = \omega_0 \frac{Z_0R}{Q_0(Z_0 + r_s)^2}. \tag{27}$$

Assuming a given r_s (determined by the circuit losses external to the junction) the gain-bandwidth product is maximum with respect to Z_0 for $Z_0 = r_s$. A well-designed circuit has low r_s (low coupling loss) and the mathcing condition derived here clearly demonstrates the importance of the microwave impedance transformer in the realization of the necessary small characteristic impedance.

At optimum the gain-bandwidth product becomes

$$G_{PA}^{1/2}\Delta\omega_{PA} = (4Z_0C)^{-1}. \tag{28}$$

Note that the only junction parameter entering Eq. (29) is the shunt capacitance which should be made as small as possible, which favors using small area tunnel junctions.

The analysis presented above deals with an ideal case which has not yet been realized in practice. So far all experiments have given bandwidth orders of magnitude less than optimum. In the experiments of Mygind *et al.*[12] there was a clear indication that the bandwidth was limited by a high Q coupling circuit. In other experiments which allegedly used broad-band input circuits the narrow bandwidth may be explained by an inadequate compensation of the series reactance which may be large if the strips leading to the small area junctions are narrow.

To illustrate the latter case we assume a constant series impedance of the form $Z_s = jX_s$ ($X_s \gg r_s$, Z_0) and find

$$G_{PA}^{1/2}\Delta\omega_{PA} = \omega_0(Z_0R/Q_0X_s^2). \tag{29}$$

The bandwidth for constant gain becomes inversely proportional to $X_s^2/Z_0 \gg Z_0$, whereas Eq. (27) predicts a bandwidth inversely proportional to Z_0 (if $r_s \to 0$). Hence a series reactance may cause a considerable bandwidth reduction.

The present discussion is valid independent of amplifier saturation in the sense that the saturation parameters have not appeared explicitly. The only assumptions were that the amplifier operating point was chosen such that the threshold condition Eq. (24) and the plasma resonance condition $\omega_R = \omega_c$ were simultaneously satisfied.

III. THE NOISE-FREE AMPLIFIER

It is helpful to investigate the performance of the ideal, noise-free, and unsaturated amplifier before we consider the more complicated general case. Even in the noise-free case the equations are complicated enough to require numerical evaluation.

The independent, external variables are the dc-bias current I_{dc} and the applied pump power P_p^+. These define the operating point (ϕ_0, α_p) via the coupled Eqs. (10), (11), (12), and (20). Given the operating point the signal power gain is determined from Eqs. (18) and (19).

Figure 2 shows the power gain at centerband using the circuit parameters listed in Table I. The centerband gain is plotted versus dc-bias current and with the pump power as a parameter (in units of RI_c^2). Centerband is defind here as a frequency infinitely close to but not coinciding with $\frac{1}{2}\omega_p$

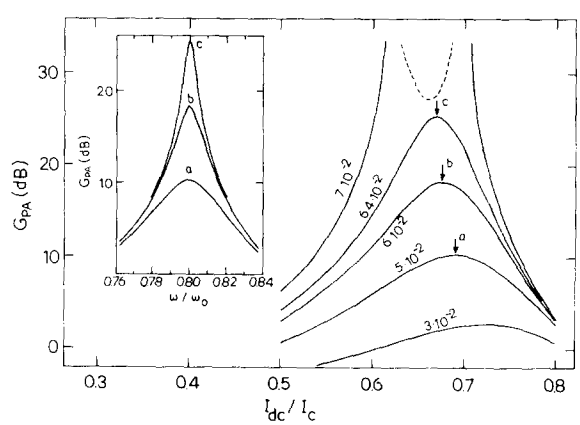

FIG. 2. Centerband gain vs dc-bias current with the pump power as a parameter (in units of RI_c^2). The inset shows the frequency response at operating points indicated by the arrows a, b, and c. The circuit parameters are given in Table I, $Z_s = r_s$.

TABLE I. The amplifier parameters used in the paper.

Junction parameters	Circuit parameters
$I_c = 200\,\mu A$	$Z_0 = 2.5\,\Omega$
$R = 10\,\Omega$	$Z_p = 2.5\,\Omega$
$\epsilon = 0$	$\omega_p = 1.6\omega_0$ [a]
	$Z_s = r_s;\quad r_s = Z_0$ [b]
$Q_0 = 10$	$= jX_s;\quad X_s = R$ [c]
	$= r_s[1 + jQ_s(\omega/\omega_s - \omega_s/\omega)];\quad r_s = Z_0, \omega_s = \frac{1}{2}\omega_p$ [d]
$\frac{\omega_0}{2\pi} = 96.6$ GHz	

[a]Except in Fig. 5.
[b]Except in Figs. 2, 8, and 11.
[c]Except in Figs. 3 and 9.
[d]Except in Figs. 4 and 10.

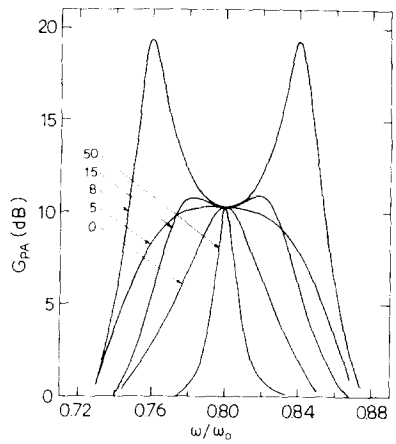

FIG. 4. Frequency response at the operating point (a) in Fig. 2, $Z_s = r_s[1 + jQ_s(\omega/\omega_s - \omega_s/\omega)]$, with Q_s as a parameter.

such that $\omega \neq \omega'$. A nonresonant and optimized coupling has been assumed ($Z_s = r_s = Z_0$).

At low pump power the centerband gain exhibits a single peak at the bias current where the plasma resonance condition is satisfied ($\omega_R = \frac{1}{2}\omega_p$). As the pump power is increased the peak gain increases towards infinity as the threshold for half-harmonic oscillation is approached. When the pump power exceeds the threshold value the gain singularity splits into two singularities which move apart as the pump power is increased further. In the dc-bias region between the two singularities the amplifier oscillates and the theory breaks down. Stable amplification requires a pump power level at some distance below the threshold, e.g., at the bias points marked by arrows. At these points the calculated frequency response is shown in the inset. The gain-bandwidth product is $0.1\omega_0$, in agreement with Eq. (27).

In order to demonstrate the effect of an uncompensated series reactance we have repeated the calculation with $Z_s = j10\,\Omega$ at the signal frequency. The remaining parameters are listed in Table I. The dependence of gain on dc-bias current shown in Fig. 3 has the same features as before. The region of positive gain has shifted towards the critical current where the plasma frequency is less than the signal frequency. This means that the capacitive part of the junction current dominates. The pump power needed to produce a given gain, e.g., 20 dB, is reduced by almost a factor of 8 compared to Fig. 2. The bandwidth is clearly degraded due to the reactance. The gain-bandwidth product is $0.02\omega_0$ from Fig. 3 whereas Eq. (29) predicts $0.025\omega_0$. (This discrepancy is understood, recalling that the condition $X_s \gg Z_0$ assumed in Eq. (29) is not satisfied.)

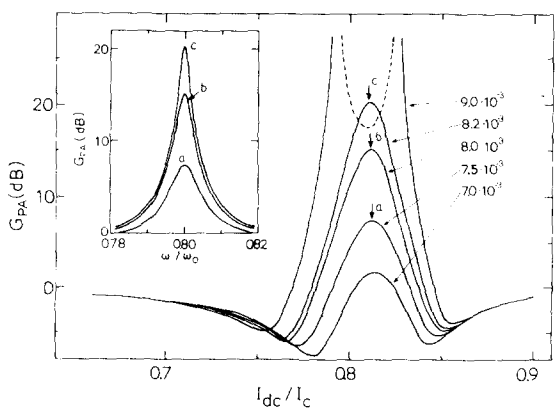

FIG. 3. Centerband gain vs dc-bias current with the pump power as a parameter (in units of RI_c^2). The inset shows the frequency response at operating points indicated by the arrows a, b, and c. The circuit parameters are given in Table I, $Z_s = jX_s$.

As a third example a single-frequency compensation of the series reactance is assumed, i.e., $X_s = 1/B_s$ at a frequency ω_s. In a narrow band centered at ω_s the series impedance (15) may be written

$$Z_s = r_s[1 + jQ_s(\omega/\omega_s - \omega_s/\omega)]. \tag{30}$$

If the centerband frequency coincides with the resonant frequency, $\omega_s = \frac{1}{2}\omega_p$, and if $Z_0 = r_s = 2.5\,\Omega$ as in Fig. 2, the centerband gain remains unchanged. The frequency response is, however, strongly modified. With a bias at the arrow "a" in Fig. 2 the gain is calculated versus frequency as shown in Fig. 4. The quality factor Q_s is used as a parameter. The trace $Q_s = 0$ repeats trace "a" in Fig. 2. As Q_s is increased from zero the bandwidth first widens. The bandwidth is increased by about a factor of 3. At intermediate values of Q_s two off-center gain peaks appear and disappear again. Only at high Q_s values the amplifier bandwidth becomes limited by the coupling circuit.

In the cases considered so far the amplifier was potentially unstable and would oscillate at pump powers above the threshold curve. At pump powers below the threshold the signal gain is very sensitive to pump power fluctuations. These properties are both eliminated if the amplifier parameters are chosen such that the threshold curve cannot be reached. One way of achieving that is to increase the pump frequency or, equivalently, to reduce the maximum plasma frequency. With $\omega_p/\omega_0 = 1.74$ and the other parameters as in Table I the centerband gain (now at $\omega/\omega_0 = 0.87$) is calculated versus dc-bias current and versus pump power. In Fig. 5(a) the result is shown versus normalized dc-bias current with pump power as a parameter and in Fig. 5(b) the param-

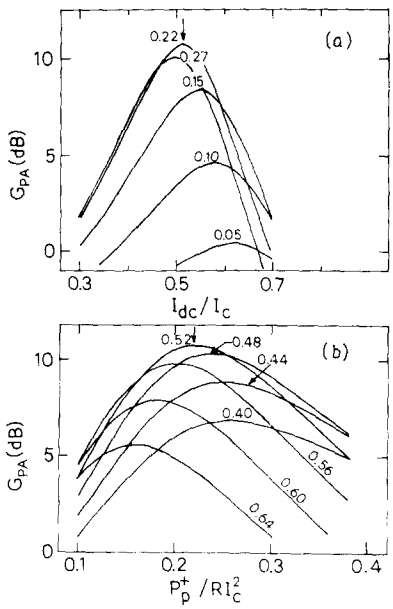

FIG. 5. (a) Centerband gain vs dc-bias current with the pump power as a parameter (in units of RI_c^2). (b) Centerband gain vs pump power with the dc-bias current as a parameter (in units of I_c). The amplifier parameters are given in Table I; $Z_s = r_s$ and $\omega_p = 1.74\omega_0$.

eters are interchanged. The pump power is measured in units of RI_c^2. The data are presented in two ways in order to clearly demonstrate that the gain may be maximized with respect to both dc-bias and pump power parameters. The optimum operating point gives a maximum gain of ~ 11 dB in this case and the gain is stable against operating point fluctuations.

Using as a measure of the stability the parameter variation necessary to produce a $\pm$ 1-dB gain change, we find 16% (10%) with respect to current and 42% (8%) with respect to pump power (the numbers in parentheses apply to Fig. 2). The gain-bandwidth product was also calculated. We found $G_{PA}^{1/2}\Delta\omega_{PA} = 0.17\omega_0$ $(0.1\omega_0)$. The improved performance is achieved at the expense of a higher pump power requirement. Compared to trace "a" in Fig. 2 we need four times as much pump power in order to obtain a gain of the order of 10 dB.

Operation at maximum gain is possible only in a narrow interval of normalized pump frequencies, as shown in Fig. 6. The maximum gain decreases rapidly as ω_p/ω_0 is increased. Operation at a gain of 10 $\pm$ 1 dB defines the pump frequency to within 0.6%. As shown in the inset the optimum operating point remains almost unchanged as the pump frequency is varied.

The calculations presented so far apply to the unsaturated amplifier and have served to illustrate some important relations. We may proceed by introducing the noise sources into the system.

IV. THE NOISE-SATURATED AMPLIFIER

A. Noise temperature—Analytical results

The noise sources to be considered here are (i) incoming blackbody radiation at a temperature T_{ext}, (ii) Johnson noise from the embedding circuit, (iii) Johnson noise from the junction resistance R, and (iv) shot noise generated by the average current flowing in the junction. The coupling circuit and the junction are assumed to be at the same temperature, T_{int}. The simple shunted junction model used here is not expected to be valid at high frequencies where the quantum corrections to the thermal noise spectra are important. Hence a classical description of the noise sources is adequate, and the fundamental photon noise limit[18] may be neglected. The quantum effects introduce in most cases only minor corrections of the classical results.

The incident blackbody radiation in an interval $d\omega$ centered at ω contributes to the junction voltage in the same way as a signal of power,

$$\overline{P_t^+(\omega)} = (1/2\pi)kT_{ext}d\omega \tag{31}$$

with the exception that the noise induced voltage is fluctuating in phase and amplitude.

The Johnson noise is taken into account by introducing a voltage source in series with Z_s with mean square amplitude

$$\overline{V_s^2(\omega)} = 2kT_{int}r_s d\omega/\pi\,, \tag{32}$$

and a current source in parallel with R

$$\overline{I_q^2(\omega)} = 2kT_{int}d\omega/\pi R\,, \tag{33}$$

The shot noise is associated with the net charge transport in the device and is given by the time average of the current flow. Since the dc current in the Josephson junction operated at zero voltage is carried by pairs of electrons we assume that this noise contribution may be given in terms of a parallel current source

$$\overline{I_p^2(\omega)} = 2eI_{dc}d\omega/\pi\,, \tag{34}$$

where the index p stands for pair. The resulting equivalent circuit model including the noise sources is shown in Fig. 7.

It is straightforward using Fig. 7 to obtain the noise power spectrum emitted from the device. In the special case that the dispersion of the series impedance Z_s is insignificant

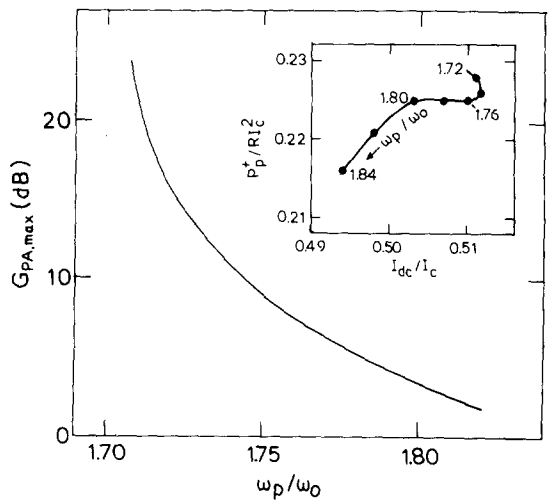

FIG. 6. Centerband gain maximized with respect to dc-bias current and pump power as a function of normalized pump frequency. The inset shows the shift in the optimum operating point as the pump frequency is varied ($\Delta\omega_p/\omega_0 = .02$ between successive solid circles).

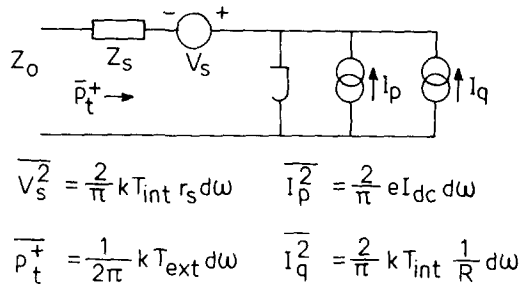

FIG. 7. Equivalent circuit with the noise sources included.

(Z_s being approximately constant over the bandwidth of the amplifier) the output noise becomes

$$\overline{P_{n,\mathrm{out}}(\omega)} = G_{PA}(\omega)\overline{P_t^+} + \tfrac{1}{2}Z_0\frac{1+|\gamma|^2}{|1+(Z_0+Z_s)Y_{\mathrm{in}}|^2} \times\left(\overline{I_q^2}+\overline{I_p^2}+\frac{\overline{V_s^2}}{|Z_0+Z_s|^2}\right), \tag{35}$$

where we have introduced $\gamma = V'^*/V$ as the ratio between idler and signal voltages. Referred to the input and excluding the incident radiation the equivalent input noise power is found by dividing Eq. (35) with the gain (18),

$$\overline{P_{n,\mathrm{in}}}(\omega) = \tfrac{1}{2}Z_0\frac{1+|\gamma|^2}{|1+(Z_s-Z_0)Y_{\mathrm{in}}|^2} \times\left(\overline{I_q^2}+\overline{I_p^2}+\frac{\overline{V_s^2}}{|Z_0+Z_s|^2}\right). \tag{36}$$

From Eq. (36) the noise temperature is found from the identity $\overline{P_{n,\mathrm{in}}(\omega)} \equiv kT_{PA}d\omega/2\pi$. Equation (36) may be simplified considerably by considering the high gain limit. In the high gain limit it may be shown that $|\gamma| = 1$, i.e., signal and idler have the same amplitude and we have $Y_{\mathrm{in}} \simeq -1/(Z_0+Z_s)$. Inserting Eqs. (32), (33), and (34) the noise temperature is found

$$T_{PA} = \frac{1}{Z_0}\left(\frac{|Z_0+Z_s|^2}{R}+r_s\right)T_{\mathrm{int}} + \frac{|Z_0+Z_s|^2}{Z_0}\frac{eI_{\mathrm{dc}}}{k}. \tag{37}$$

Obviously the impedance relation $|Z_0+Z_s|^2/Z_0$ should be minimized. For given Z_s the noise temperature is minimum for $Z_0 = |Z_s|$ with a minimum value

$$T_{PA}^{\min} = \left(\frac{2(|Z_s|+r_s)}{R}+\frac{r_s}{|Z_s|}\right)T_{\mathrm{int}} + 2(|Z_s|+r_s)\frac{eI_{\mathrm{dc}}}{k}. \tag{38}$$

This result clearly demonstrates that (i) a large junction resistance is preferable, (ii) a series reactance jX_s may easily degrade the performance also in terms of noise temperatures, (iii) in the case $Z_s = r_s$ the minimum noise temperature is obtained if $Z_0 = r_s$ which simultaneously maximizes the gain-bandwidth product, (iv) the shot noise contribution may be written $2(|Z_s|+r_s)(eRI_c/k)(I_{\mathrm{dc}}/I_c)/R$, where eRI_c/k typically is ~ 12 K ($e/k = 11.6$ K/mV), and (v) the thermal noise follows the ambient temperature T_{int}, whereas the shot noise decreases as the device temperature is raised.[19] For certain circuit and junction parameters an optimum operating temperature may exist which minimizes the overall junction noise.

B. Noise and signal saturation

In the series expansion (1) of the junction voltage each frequency is represented by one term, whereas we have introduced four different noise sources all contributing at any given frequency. However, any number of terms in Eq. (1) may have coinciding frequencies if only their amplitudes and phases are incoherent as is the case of noise contributions derived from independent sources.

The saturation parameters (5) and (5') may be expressed in terms of mean square junction voltages. Using Eq. (3')

$$A = \sum_k (2e/\hbar\omega_k)^2[1+(\omega_k/\omega_k')|\gamma_k|^2]\overline{|V_k|^2},$$
$$B = \sum_k (2e/\hbar)^2(\gamma_k^*/\omega_k\omega_k')\overline{|V_k|^2}, \tag{39}$$
$$\gamma_k \equiv \frac{V_k'^*}{V_k} = -Y_{21}(Z_s'^*+Z_0)/[1+Y_{22}(Z_s'^*+Z_0)],$$

where the mean square junction voltage is determined from the equivalent circuit model in Fig. 7,

$$\overline{|V_k|^2} = \frac{8Z_0\overline{P_t^+}+\overline{V_s^2}+(Z_0+Z_s)^2(\overline{I_q^2}+\overline{I_p^2})}{|1+(Z_0+Z_s)Y_{\mathrm{in}}|^2}. \tag{40}$$

The equations (10)–(14), (19), (20), (39), and (40), which determine the operating point of the saturated amplifier, are all interdependent and must be solved self-consistently. The iteration procedure outlined below may be used. The procedure relies on the observation that although A and B may not have reached their final values at some stage in the iterative process the ratio B/A converges rapidly.

The theoretical evaluation assumes small values of A and B, and a convenient initial guess is $A_i = 0$, $B_i = 0$. The iteration then proceeds: (i) With initial values $A_n = A_i$, $B_n = B_i$, Eqs. (10), (11), and (20) are solved for (ϕ_0, α_p) with given independent variables I_{dc} and P_p^+. (ii) The matrix elements Y_{ij} are calculated from Eq. (14) for each frequency ω_k, and the input admittance Y_{in} is calculated from Eq. (19) as a function of frequency. (iii) The junction voltage components $\overline{|V_k|^2}$ are calculated from Eqs. (40) and (31)–(34). (iv) New values A_{n+1}, B_{n+1} are determined from Eq. (39). (v) If $A_{n+1} = A_n$ and $B_{n+1} = B_n$, the iteration has converged. This is tested by calculating I_{dc} and P_p^+. If the result is self-consistent, all amplifier properties may be evaluated. (vi) If the iteration has not converged a new set of initial values are chosen. Either, by increasing A_i in steps with $B_i = (B_{n+1})/A_{n+1})A_i$ until a sign change in the function $f(A_n) = A_n - A_{n-1}$ is localized. Or, by linear interpolation, $A_i = [f(A_{n+1})A_n - f(A_n)A_{n+1}]/[f(A_{n+1}) - f(A_n)]$, if $f(A_{n+1})f(A_n) < 0$. (vii) In either case the sequence (i) to (v) is repeated until the prescribed accuracy is obtained.

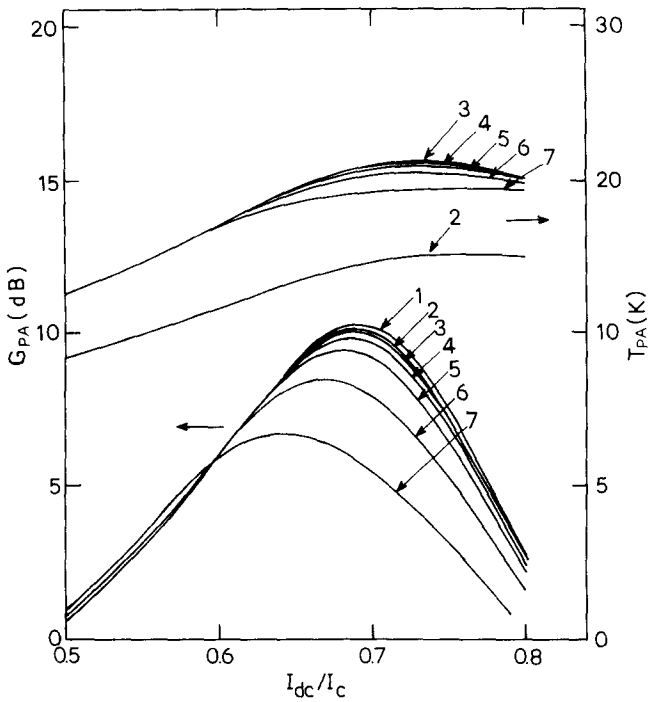

FIG. 8. Centerband gain (lower traces, left-hand scale) and noise temperature (upper traces, right-hand scale) vs dc-bias current. $P_p^+ = 5\times10^{-2}$ RI_c^2. Trace 1: Noise-free case; trace 2: shot noise only; traces 3–7: shot noise and internal noise with $T_{int} = 4.2$ K; $T_{ext} = 0$, 10, 30, 100, and 300 K, respectively.

Following this procedure the results shown in Fig. 8 have been calculated. The centerband gain and the noise temperature are shown versus dc-bias current using the circuit parameters listed in Table I. Trace 1 is identical to trace "a" in Fig. 2. In trace 2 only the shot noise has been included ($T_{int} = T_{ext} = 0$ K). Finally, traces 3–7 are calculated with all noise sources contributing, $T_{int} = 4.2$ K, and $T_{ext} = 0$, 10, 30, 100, and 300 K, respectively. As the temperature of the incoming blackbody radiation is increased the maximum gain is suppressed considerably. A suppression of almost 4 dB results when 300 K radiation is applied. At the same time the gain peak shifts in current. The noise temperature shown in the upper half of Fig. 8 (the right-hand scale) is almost independent of the incoming noise as we should expect from Eq. (38). The noise temperature does, however, decrease slowly as T_{ext} increases because the saturation violates the condition of high gain assumed in Eq. (38).

With an uncompensated reactive coupling impedance $Z_s = j10\ \Omega$ at centerband the results shown in Fig. 9 are found. The pump power is adjusted to give an unsaturated gain of 10 dB and all the other parameters are as in Fig. 3. The saturation is stronger than in Fig. 8. Even incoming radiation at a temperature of 100 K (trace 6) produces a gain suppression of 5 dB. Compared to Fig. 8 the noise temperature has increased by an order of magnitude and a strong dc-bias current dependence is apparent. The noise temperature traces show a pronounded double peak structure with a minimum at the bias where the gain peaks. The maxima in the noise temperature is a reflection of the gain minima flanking the gain peak The output noise varies smoothly with current with a single maximum at maximum gain.

The comparison between Figs. 8 and 9 corroborates further that the elimination of the series inductance is very important.

The effect of a simple, single-frequency compensation on the saturation and on the noise temperature is illustrated in Fig. 10. With a series impedance of the form Eq. (30) and the system parameters given in Table I the gain and the noise temperature are calculated versus T_{ext} using Q_s as a parameter.

For each Q_s the dc-bias point is kept fixed at the value corresponding to maximum gain for $T_{ext} = 0$ K and $T_{int} = 4.2$ K. The pump power is adjusted to given an unsaturated gain of 10 dB. Some saturation is present already at $T_{ext} = 0$ K due to the internal noise sources. The main features of Fig. 10 are as follows: As Q_s is increased the saturation at first gets worse. This may be understood with reference to Fig. 4 which showed that by narrowing the passband of the input circuit the amplifier bandwidth increased. Hence the integrated noise power becomes larger and a stronger saturation is the result. At intermediate values of Q_s the situation becomes more complicated. The amplifier response becomes

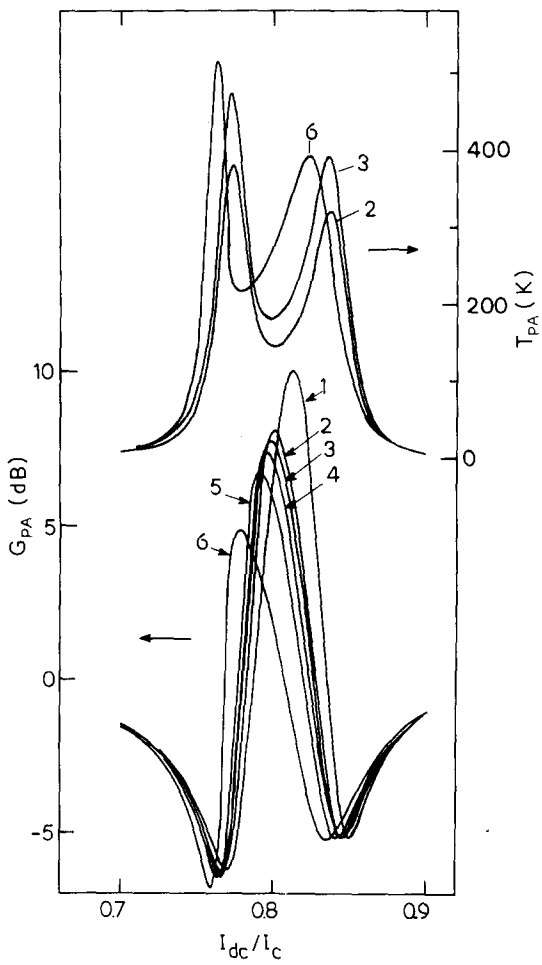

FIG. 9. Centerband gain (lower traces, left-hand scale) and noise temperature (upper traces, right-hand scale) vs dc-bias current. $P_p^+ = 7.7\times10^{-3}$ RI_c^2. Trace 1: Noise-free case; trace 2: shot noise only, traces 3–6: shot noise and internal noise with $T_{int} = 4.2$ K; $T_{ext} = 0$, 10, 30, and 100 K, respectively. Amplifier parameters as in Fig. 3.

re-entrant, demonstrating that the response is the outcome of an active interaction between the correlated gain, bandwidth, and noise power. The low gain branch of the double valued trace is, however, so strongly saturated ($A \simeq 0.4$) that the theory is no longer accurate. At high values of Q_s the coupling circuit starts to limit the effective bandwidth and the gain saturation is reduced.

The noise temperature shown in the upper part of the figure repeats the behavior on a much compressed scale. The general tendency is that the noise temperature is reduced as the amplifier becomes saturated, but the total variation does not exceed 20%.

As mentioned in Sec. II the theory may account for signal saturation as well as for noise saturation. To illustrate this point we have calculated gain and noise temperature versus input signal power at the amplifier center frequency. The amplifier parameter are as listed in Table I. The junction operates at a temperature of $T_{\text{int}} = 4.2$ K and the signal is assumed noise free ($T_{\text{ext}} = 0$ K). In the upper part of Fig. 11 the resulting gain and noise temperature are shown. In the lower part the same data are plotted in terms of output quantities assuming that the bandwidth is limited to 1 MHz by a subsequent detector stage (according to Fig. 2, trace "a" the

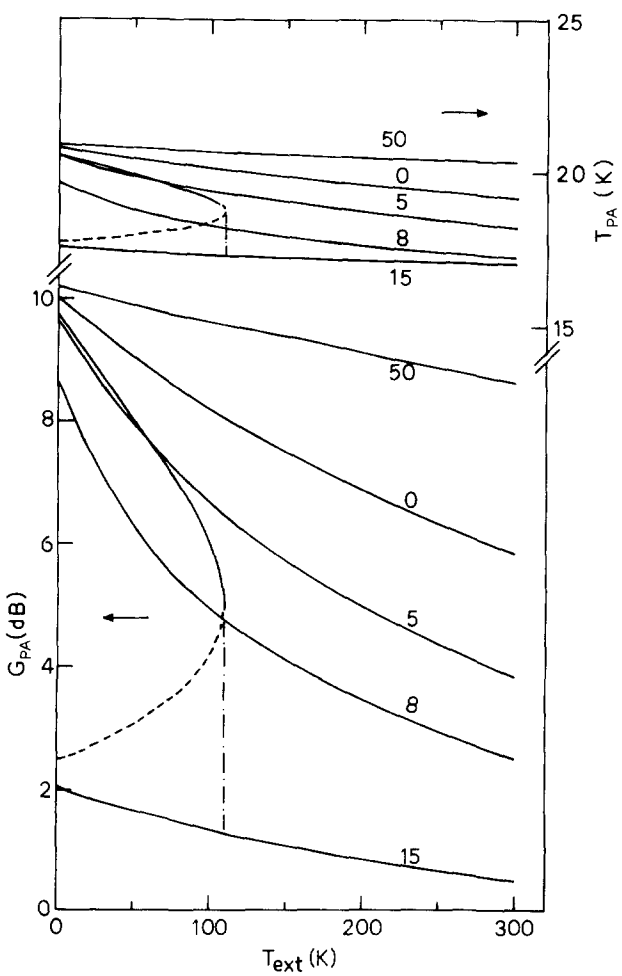

FIG. 10. Centerband gain (lower traces, left-hand scale) and noise temperature (upper traces, right-hand scale) vs temperature of incoming blackbody radiation and with the quality factor Q_s of the resonant input circuit as a parameter. Amplifier parameters as in Fig. 4.

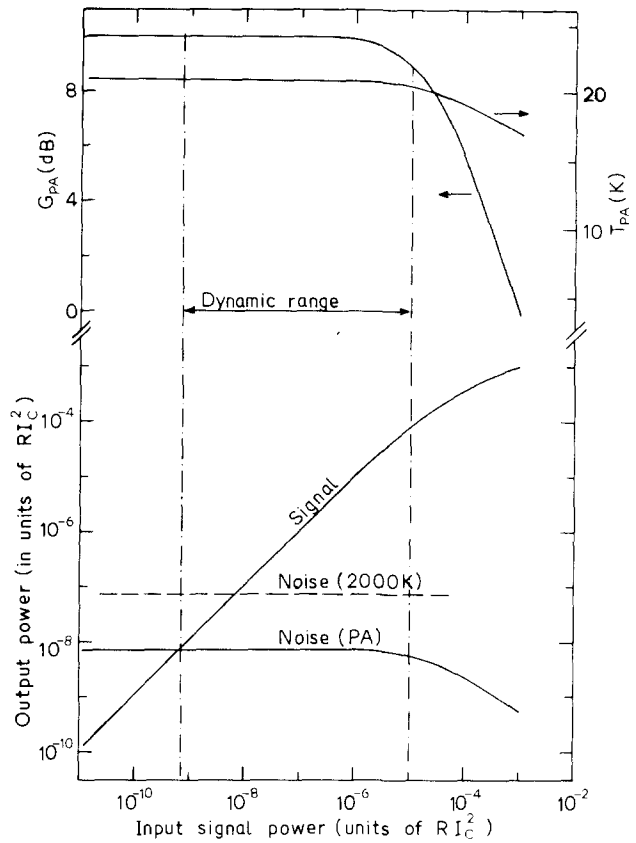

FIG. 11. Centerband gain and noise temperature vs input signal power (upper part, left- and right-hand scales, respectively). Output power vs input signal power (lower part). They dynamic range is defined as the distance between the 1-dB gain compression point and the point of unit signal-to-noise ratio ($S/N = 1$). The horizontal dashed line calibrates the power axis in terms of temperature (white noise at 2000 K in a 1-MHz bandwidth).

unsaturated amplifier bandwidth is ~ 1 GHz). The useful dynamic range of the present amplifier is found from Fig. 11. The minimum detectable power ($S/N = 1$) is $\sim 7 \times 10^{-10}$ and the maximum power is $\sim 10^{-5}$ using the 1-dB gain compression point as an upper limit. The power is measured in units of $RI_c^2 = 0.4\,\mu$W. A reference in terms of output temperature is given by the dashed horizontal line representing white noise at 2000 K in a 1-MHz bandwidth. This noise level might represent the SSB noise temperature of a good quality room-temperature mixer stage.

V. SUMMARY

The present theory of the singly quasidegenerate Josephson junction parametric amplifier relies on the applicability of the phenomenological shunted junction model, which does not take into account the frequency dependence of the pair and quasiparticle currents. Nevertheless, a large variety of experimental observations have been successfully interpreted in terms of this simple model and we believe that meaningful results may be derived also in the present context.

All the high-frequency excitations except the pump are treated as weak signals. A description of the amplifier response in terms of (nonlinear) admittances at each of the

frequencies involved is then possible. Evaluation of the circuit equations to third order in the weak signals gives the lowest-order self-consistent account of amplifier saturation effects. Formally, the saturation is expressed in terms of amplitude-dependent admittance elements, i.e., the admittance seen at a particular frequency depends on the signal amplitudes at every other frequency.

Only weak excitations at frequencies in a band centered at half the pump frequency is included, since here the device may be parametrically active in the singly degenerate mode and the signals may build up to appreciable amplitudes. Except at the pump frequency the junction admittance is assumed infinite outside this band. This approximation is reasonable if the Josephson plasma resonance has a high Q. Below resonance the junction is shorted by the pair current, and above resonance the capacitive displacement current short circuits the junction. Only at resonance is it possible to induce a voltage across the junction, and the plasma resonance therefore must be tuned to coincide with half the pump frequency in order to realize parametric gain in the mode considered here.

The treatment of the pump frequency component is not quite consistent with these ideas. Assuming that the pump signal is supplied from a loss-free line characterized by a real waveguide impedance, we have implicitly implied that all reactive elements in the pump input circuit have been resonated out. We have not, however, put much emphasis on the coupling to the pump and have accordingly avoided to compare saturation power levels to applied pump power. We want to emphasize, however, that great care must be exerted when designing pump circuits if the potentially very low pump power requirements are crucial to a particular application.

Saturation due to signal or noise is included. The noise may be generated in or outside the junction. External noise sources considered are (i) blackbody radiation reaching the junction via the input lines and (ii) thermal (Johnson) noise from dissipative elements in the embedding circuit. Internal noise sources are (i) thermal (Johnson) noise in the junction quasiparticle resistance and (ii) shot noise determined by the net current flow (carried by pairs). The strengths of the individual noise sources are described classically, primarily justified by the high-frequency limitations already inherent in the shunted junction model, and secondarily because the obvious quantum corrections (the Planck distributions of the black body radiation and the photon shot noise in most cases would be of minor importance. A closed form expression for the spectral density of the quasiparticle noise has been derived[20] which at low frequencies reproduces the classical Johnson noise spectrum and at high frequencies goes into a shot-noiselike expression. The pair noise spectrum has been derived only at finite dc-voltages and the expression diverges at zero voltage[21] which is clearly unphysical. Therefore we decided to perform a classical noise analysis which we believe gives a conservative estimate of the junction noise.

The final problem addressed in order to develope a realistic model is the influence of the embedding microwave circuit. In the present discussion the coupling circuit is represented by an LC-resonance circuit in series with the junction. An ideal impedance transformer is also included in the signal input line since reduction of the characteristic waveguide impedance is crucial for the proper performance of the device. Using this circuit a number of realistic situations are modeled going from an uncompensated series reactance over a narrow band to broad-band compensation of the input circuit series reactances.

In the high gain limit amplifier properties such as the gain-bandwidth product and the noise temperature are found in closed analytical form provided that the dispersion of the coupling circuit is negligible over the bandwidth of the amplifier. In the general case only a numerical approach is feasible. In order to solve the coupled circuit equations self-consistently an iteration procedure is developed which in most cases converges rapidly.

Using analytical and numerical methods we found that the optimum performance in terms of maximum gain-bandwidth product and minimum noise temperature is achieved by matching the waveguide impedance to the circuit losses represented by a resistance in series with the junction. Minimizing the coupling circuit losses further improves the performance. This result is based on the idealized situation that the external circuit is nonreactive. The presence of an uncompensated series reactance deteriorates the amplifier response. It decreases the gain-bandwidth product, increases the noise temperature, and causes the amplifier to saturate more easily. A large junction resistance reduces these problems. The device noise temperature and the saturation due to internal noise are reduced as the junction resistance is increased.

High-frequency applications require junctions with a high maximum plasma frequency, and hence a large supercurrent density. This requirement is only compatible with the demand for a large junction resistance and a small junction capacitance [c.f. Eq. (28)] if the junction area is small.

Noise saturation due to external sources may be reduced by a bandpass filter, e.g., a Q filter in the input line. The passband of the filter should, however, be much less than the intrinsic bandwidth of the amplifier (defining the latter with an infinite bandwidth input circuit). For filter Q's comparable to that of the amplifier the combined bandwidth is found to increase over the intrinsic amplifier bandwidth and a complicated re-entrant gain is found in some cases.

An alternative method to reduce the saturation caused by incoming broad-band or monochromatic radiation is to use an array of identical junctions, since the available power is shared evenly between the individual junctions.[22] It is, however, not obvious how the array will respond to noise from internal sources. Each junction contributes to the system noise and the saturation produced by the internal noise sources may not depend drastically on the number of junctions. The noise power delivered to the external load is a complicated function of the loading of each junction in the presence of the others. This problem has not yet been solved, and we cannot predict the noise temperature or the dynamic range of an amplifier using a junction array.

In the X-band experiments on a single tunnel junction amplifier[11] we found noise temperatures of the order of several thousand degrees. The circuit parameters were far from

optimum ($R \ll Z_0$, r_s) and high noise temperatures should be expected. However, the theory does not apply to this case since the presence of large amplitude fluctuations in the junction voltage would produce strong saturation and violate the assumption $A \ll 1$. In the 35-GHz experiments we had $R > Z_0$ and low noise temperatures were measured.[12] We believe that the excessive amplifier noise which is often observed is closely correlated with the growth of the half-harmonic amplitude as the operating point approaches the gain instability threshold. We defer from a further discussion of this problem which clearly cannot be solved within the framework of the present theory.

VI. CONCLUSION

In conclusion we repeat the main results of the theory. In order to optimize the performance of the singly quasidegenerate Josephson junction parametric amplifier the following points deserve special attention.

(i) The coupling circuit represented by a series impedance Z_s should match the characteristic impedance Z_0 of the input/output waveguide line, i.e., $\mathrm{Im}Z_s = 0$ and $\mathrm{Re}Z_s = Z_0$ at the signal frequency. The coupling loss represented by $r_s = \mathrm{Re}Z_s$ should preferably be small. Hence it is crucial to employ an impedance transformation in order to realize the impedance matching to standard waveguides. The reactance $\mathrm{Im}Z_s$ includes the parasitic inductance of the Josephson junction structure which must be resonated out by the expediency of introducing another reactive structure at an appropriate location in the waveguide.

(ii) The junction resistance R should be larger than Z_0 and the junction capacitance C should be small. Furthermore, the maximum Josephson plasma frequency ω_0 must be greater than the signal frequency. These three quantities are related by the equation $\omega_0^2 RC = 2eRI_c/\hbar$, where the right-hand side is a materials constant, ($2eRI_c/\hbar = \pi\Delta/\hbar$ at $T = 0$ K, where Δ is the superconducting energy gap of the electrode material).

(iii) The amplifier may be saturated by low levels of input power and even by noise from internal sources. The degree of saturation due to incoming and internally generated noise may be reduced by introducing a narrow-band filter in the input/output waveguide.

(iv) The noise temperature is dominated by internal noise sources and virtually independent of incoming blackbody radiation. Hence the noise temperature cannot be reduced by using a narrow-band input filter.

So far no attempts have been made to test the theory against existing experimental results.[11,12] In order to do that it is crucial that the microwave circuit is known in every detail. However, most of the observed properties may be accounted for in a qualitative way within the framework of the theory.

The theory presented here applies explicitly to the singly quasidegenerate amplifier. We believe, however, that an equally detailed theory including a realistic coupling circuit and internal noise sources for the doubly degenerate, or SUPARAMP, mode will lead to similar conclusions. Complications may arise since the pump power is supplied through a common signal, idler, and pump circuit, which imposes additional constraints on the circuit components.

ACKNOWLEDGMENT

This work was supported in part by The Danish Natural Science Research Council, grant no. 511-15059.

[1] A. N. Vystavkin, V. N. Gubankov, L. S. Kuzmin, K. K. Likharev, V. V. Migulin, and V. K. Semenov, IEEE Trans. Magn. **MAG-13**, 233 (1977).
[2] L. S. Kuzmin, K. K. Likharev, and V. V. Migulin, IEEE Trans Magn. **MAG-15**, 454 (1979).
[3] P. T. Parrish and R. Y. Chiao, Appl. Phys. Lett. **25**, 627 (1974).
[4] R. Y. Chiao and P. T. Parrish, J. Appl. Phys. **47**, 2639 (1976).
[5] S. Wahlsten, S. Rudner, and T. Claeson, J. Appl. Phys. **49**, 4248 (1978).
[6] F. Goodall, F. Bale, S. Rudner, T. Claeson, and T. F. Finnegan, IEEE Trans. Magn. **MAG-15**, 458 (1979).
[7] Y. Taur and P. L. Richards, J. Appl. Phys. **48**, 1321 (1977).
[8] M. J. Feldman, P. T. Parrish, and R. Y. Chiao, J. Appl. Phys. **46**, 4031 (1975).
[9] M. J. Feldman, J. Appl. Phys. **48**, 1301 (1977).
[10] D. W. Peterson, Ph. D. thesis, University of California, Berkeley, 1978; R. Y. Chiao, M. J. Feldman, D. W. Peterson, B. A. Tucker, and M. T. Levinsen, AIP Conf. Proc. **44**, 259 (1978).
[11] J. Mygind, N. F. Pedersen, O. H. Soerensen, Appl. Phys. Lett. **32**, 70 (1978).
[12] J. Mygind, N. F. Pedersen, O. H. Soerensen, B. Dueholm, and M. T. Levinsen, Appl. Phys. Lett. **35**, 91 (1979).
[13] V. N. Belykh, N. F. Pedersen, and O. H. Soerensen, Phys. Rev. B **16**, 4853 and 4860 (1977).
[14] N. F. Pedersen, O. H. Soerensen, B. Dueholm, and J. Mygind, J. Low Temp. Phys. **38**, 1 (1980).
[15] N. Markuvitz, *Waveguide Handbook* (Dover, New York, 1965), p. 221.
[16] A. Farrar and A. T. Adams, IEEE Trans. Microwave Theory Tech. **MTT-20**, 497 (1972); P. Benedek and P. Sylvester, IEEE Trans. Microwave Theory Tech. **MTT-20**, 729 (1972).
[17] With a high Q resonant coupling circuit the condition of infinite gain may be satisfied at frequencies different from $\omega_c = \frac{1}{2}\omega_p$. In experiments we have observed amplifier oscillations at two (occasionally three) frequencies simultaneously. These frequencies satisfied $\omega_1 + \omega_2 = \omega_p$, ($\omega_3 = \frac{1}{2}\omega_p$).
[18] W. H. Louisell, A. Yariv, and A. E. Siegman, Phys. Rev. **124**, 1646 (1961).
[19] Not only does the RI_c product decrease as the sample temperature is raised, also the bias current I_{dc}/I_c should be reduced in order to satisfy the plasma resonance condition as the maximum plasma frequency decreases.
[20] A. J. Dahm, A. Denestein, D. N. Langenberg, W. H. Parker, D. Rogovin, and D. J. Scalapino, Phys. Rev. Lett. **22**, 1416 (1969).
[21] M. J. Stephen, Phys. Rev. **182**, 531 (1969).
[22] The response of an N-junction array to external excitations may be calculated from the equations in this paper by replacing the junction admittance matrix (Y_{ij}) by $(Y_{ij})/N$.